Hindawi
International Journal of Polymer Science
Volume 2023, Article ID 7927196, 13 pages
https://doi.org/10.1155/2023/7927196

Research Article

Acquisition of Key Vacuum-Assisted Resin Transfer Molding Parameters through Reverse Scanning for Application in the Manufacturing of Large Fiber-Reinforced-Plastic Products

Guang-Min Luo,[1] Kai-Lin Chen ,[2] and Chen-Ting Hsu[1]

[1]*Department of Naval Architecture and Ocean Engineering, National Kaohsiung University of Science and Technology, Kaohsiung, Taiwan*
[2]*Ph.D. Program in Maritime Science and Technology, National Kaohsiung University of Science and Technology, Kaohsiung, Taiwan*

Correspondence should be addressed to Kai-Lin Chen; i109188102@nkust.edu.tw

Received 4 April 2023; Revised 9 May 2023; Accepted 13 May 2023; Published 23 May 2023

Academic Editor: Voon-Loong Wong

Software-based mold flow analysis is often performed to confirm optimized resin pipe arrangements. In this study, the GeoDict software and reverse scanning were employed to develop a method for performing rapid porosity and permeability estimation. A comparison of the results from one-dimensional resin flow and Easyperm tests revealed a 10% variation in the porosity and permeability parameters obtained through the proposed rapid estimation method. In addition, the obtained parameters were substituted into a Moldex3D model to simulate the resin flow on the personal watercraft hull during vacuum-assisted resin transfer molding (VARTM). A comparison of simulation results and hull infusion results revealed that the integration of the proposed rapid estimation method with Moldex3D allowed for the accurate simulation of the resin flow in large fiber-reinforced-plastic (FRP) products (variation <8%). The proposed method can be applied to large wind turbine FRP parts and large FRP yacht components to increase process planning efficiency and product stability.

1. Introduction

Vacuum-assisted resin transfer molding (VARTM) is the most widely used technique for manufacturing large fiber-reinforced-plastic (FRP) components. The application of closed molding in VARTM to manufacture large FRP components (>10 m) reduces the cost of manufacturing and increases the competitiveness of a manufacturer in the composites market. This method has been widely used to manufacture wind turbine components and structures, including wind blades, nacelle covers, and nose cone covers [1, 2]. The dimensions of these components range from 10 to 115 m, and the thickness of components subjected to a single infusion can reach 10–20 cm. Because the thickness and size of such products are considerably large, manufacturers must confirm that all the empty spaces between and within fiber tows have been filled with resin before resin curing. Therefore, the fluid mechanics of the resin impregnating the fabrics and curing characteristics of this resin are key factors of the manufacturing process. Bodaghi et al. [3] consolidated the relevant research findings reported in the past 30 years and identified the parameters that affect resin flow characteristics during the infusion process and the interrelationship between these parameters. An increase in porosity causes resin flow to accelerate but also affects various mechanical properties. During the process of designing FRP parts, structural properties tend to be the main focus, whereas problems pertaining to resin fluid mechanics tend to be overlooked. Accordingly, a method for quickly estimating the permeability of fabrics must be developed to establish a database of the resin flow characteristics of various fabrics.

Fabric permeability has been extensively studied, and the one-dimensional resin flow test is the most commonly used method for assessing fabric permeability. Parnas et al. [4],

Amico and Lekakou [5], and Tan and Pillai [6] performed one-dimensional resin flow tests to study the permeability of woven fabrics, plain weave fabrics, and non-crimp fabrics (NCFs). In addition to the one-dimensional resin flow test, other permeability estimation methods have been proposed. Nabovati et al. [7] applied the lattice Boltzmann method to simulate and predict the permeability of woven fabrics, and Wang et al. [8] applied a conventional modeling method to predict permeability. In addition, Endruweit et al. [9] used the radial flow experimental method to explore the relationship between pressure and porosity in biaxial fabrics. Regarding the performance of VARTM, Han et al. [10] and Kang et al. [11] conducted one-dimensional flow tests to examine the relationship between thickness and pressure variations. Correia et al. [12] studied the differences in the numerical model simulation results obtained for single- and double-sided rigid molds. Their research results indicate that in single-sided rigid molds, the compaction effect between fabrics under vacuum compression reduces fabric permeability and porosity, which increases resin flow time. Buntain and Bickerton [13] used a compressible mechanism for continuous measurement to verify the relationship between permeability and porosity. Govignon et al. [14] applied digital speckle stereo photogrammetry to clarify the associations between fabric thickness, porosity, and permeability under various lamination sequence during the infusion process. Mogavero and Advani [15] observed resin flow characteristics under various fabric thicknesses and lamination conditions. Collectively, the aforementioned literature findings indicate that fabric thickness, porosity, and permeability are the main parameters that influence resin flow time when resin is flowing in fabrics.

To increase the efficiency of obtaining parameters, Caglar et al. [16] used two-dimensional sections to predict permeability in a three-dimensional model. To verify the differences in permeability test results, Arbter et al. [17] examined 11 units and applied 16 test procedures to obtain parameters from their test results. Thereafter, they compared the differences in various parameters and reported that relative to nonpersonal errors, personal errors may lead to twice as many permeability variations. Liu et al. [18] measured the in-plane permeability of 3/1 twill weave, 2/2 twill weave, and plain weave by using the built-in electrical sensor of a mold. Their results indicate that K_x and K_y, which represent in-plane permeability, are only significantly correlated for some woven fabrics. Because most studies have only focused on global material properties and overlooked the local characteristics of flow behaviors, Chiu et al. [19] used a pressure sensor array measurement system to measure the local variability of the ratio of permeability to porosity, and they used this result as the input parameter for the local flow characteristics applied in a simulation and flow control. The technical data sheets (TDSs) of fabrics state that a fabric might exhibit areal density variations of approximately ±10% during its production. When fabrics are laminated to manufacture finished products, their overall porosity variation might change depending on the laminated sequence; this phenomenon increases the difficulty of predicting the resin flow in fabrics and hinders the establishment of a parameter database for resin flow. Therefore, the establishment of a low-variation, rapid method for predicting parameters, such as porosity, permeability, and thickness, can contribute toward the establishment of a database for resin flow characteristics.

Moreover, to improve the process stability and reduce the risk involved in using VARTM to produce large structural FRP parts, mold flow analysis software is often used to conduct resin flow simulation and process planning before infusion. Mold flow analysis results are used as the basis for optimizing the location of piping, thereby reducing the risk of product infusion failure. Mold flow analysis is based on Darcy's law, which posits that the resin flow front is a function of permeability that is driven by a fixed pressure. For traditional permeability measurements, permeability parameters must be obtained through a one-dimensional resin flow test or permeability measurement equipment. However, because the area density of every single fabric has variations and fabric weaving process also makes the spacing of each strand of glass filament inconsistent, these variations are the factors to influence permeability and porosity. To obtain averaged parameters pertaining to each batch of fabric permeability and porosity, multiple tests must be conducted and considerable resources must be spent on testing.

Currently, commercially available mold flow analysis packages include Moldex3D, Polyworx, PAM-RTM, and various equivalent simulation tools. Wei et al. [20] used Moldex3D to perform mold flow analysis and compared their experimental results. Härter et al. [21] used PAM-RTM for simulations; they also used a mold design and various fabrics to solve the resin flow and infusion problems that are attributable to K_z being much smaller than the in-plane permeability of the fabrics. Trochu et al. [22] used RTMFLOT to simulate the infusion of a lawn mower hood, and they tested various injection port positions, air vents positions, and injection pressure levels to optimize their cycle time. Dong [23] applied the traditional method and equivalent medium method to simulate the infusion conditions of the cover plate of an unmanned aerial vehicle. Their research results reveal that the equivalent medium method considerably reduced the time required for mold flow analysis. Parseval et al. [24] confirmed that the resin flow within fiber tows is incompressible flow [i.e., constant-density flow involving a Newtonian fluid (liquid with constant viscosity)]. Therefore, viscosity variations need not be considered during mold flow analysis. However, the variations in fabric porosity and thickness must be considered. Droste et al. [25] developed a noncontact method for measuring fabric thickness variation during resin flow and for assessing the fabric compaction status pertaining to various fabrics layers. However, Bodaghi et al. [26] and Rodriguez et al. [27] have highlighted that parameters, such as porosity and permeability, vary substantially because of fabric weaving and the sequence of fabric compositions. Therefore, a database of resin flow characteristics, such as permeability and porosity, pertaining to various fabrics must be established. Dong [28] used the design-of-experiments method to identify flow parameters. Furthermore, they used a three-dimensional

model for simulation, and the variation between the experimental and simulation results for a car hood was <15%.

Permeability and porosity are crucial input parameters in mold flow analysis. With the support of 13 academic units, Vernet et al. [29] conducted in-plane permeability measurement experiments under fixed conditions with respect to fiber content, infusion pressure, and resin viscosity. Their experiments revealed a maximum permeability variation of 20%, and the factor of variation was verified to be mainly driven by the differences between experimental procedures. However, in industrial production, a gap between mold flow analysis results and practical resin infusion outcomes often exists. This gap is inferred from our practical manufacturing experiences that could mainly cause by the inaccurate measurement of fabric porosity and permeability.

In the present study, the GeoDict software and reverse scanning, a process that involves measuring a physical object and reconstructing it as a 3D model to recover the design intent, were employed to develop a method for rapidly estimating fiber porosity and permeability. Under fixed lamination conditions, flat specimens were produced through VARTM, after which a computed tomography (CT) scanning was performed to obtain the ratio of resin to fabric in the laminated section. Next, the GeoDict software was used to construct an image to determine the porosity and permeability under these lamination conditions. To verify the accuracy of the proposed method, a one-dimensional resin flow test and the Easyperm system were used to compare the obtained permeability parameters. A personal watercraft (PWC) hull was also used as a target in a practical experiment. Moldex3D was applied to simulate the resin flow in a large mold. Finally, the obtained parameters were then applied in an infusion simulation of a PWC hull. Subsequently, we compared the simulation and practical infusion results to verify the applicability of the proposed rapid estimation method. When VARTM is performed to produce large FRP products, the proposed rapid estimation method can be applied to obtain porosity and permeability, which are required for mold flow analysis.

2. Methods for Measuring Mold Flow Parameters

Three methods were used to obtain porosity, permeability, and thickness: the traditional one-dimensional flow test; measurement with the Easyperm system, which was developed by the ESI Group to measure permeability; and the proposed rapid permeability estimation method, which mainly involves using WeaveGeo and FiberGeo in GeoDict for three-dimensional modeling and adopting a FlowDict module for analysis and the acquisition of various parameters.

In the one-dimensional flow test, we assessed the relationship between the flow front and flow time of the resin and applied Darcy's law to obtain the resin flow permeability K after determining viscosity and porosity. VARTM was the manufacturing process examined. To evaluate the porosity of a fabric, it must be stacked under vacuum conditions to measure its thickness. Fabric porosity (ϕ_f) is obtained using the following equation [30]:

$$\phi_f = 1 - \frac{\rho_{fs} \times A_f / \rho_f}{A_f \times t_f}, \tag{1}$$

where t_f is the fabric thickness under vacuum conditions, ρ_{fs} is the areal density, ρ_f is the fiber density, and A_f is the area within which fabrics are laid.

To estimate the permeability of fabrics, they were cut into $15 \times 50\,cm^2$ pieces and laminated on the basis of the number of layers to be measured. After each piece completed infusion, the relationship between the flow front and flow time of the resin was assessed, and the permeability K of the laminate was obtained using the following equation [31]:

$$K = \frac{\phi_f \times \mu}{2 \times \Delta P} m, \tag{2}$$

where μ is the resin viscosity, which must be measured using a viscometer in a thermostatic water bath; ϕ_f is the porosity, which is obtained using equation (1); ΔP is the vacuum pressure gradient, which was assumed to be −1 bar in this study; and m is the slope of the square of the resin flow front versus the resin flow time. After all the required parameters were obtained, the permeability K of the fabrics under lamination conditions was obtained using equation (2).

After performing the one-dimensional flow test, the permeability of fabrics was measured using the Easyperm system, which is a professional permeability measurement instrument developed by the ESI Group in Rungis, France (Figure 1). Easyperm is a pressure control system that mainly uses a network of pressure sensors to measure resin flow rates and partial pressure variations in multiple areas. This instrument is equipped with six pressure sensors, which can record the partial pressure at each observation point, the pressure variation over time, and the duration of resin flow front arrivals. Finally, the saturated permeability of the resin flowing in a fabric can be obtained by combining the following equations [32]:

$$K_{ii} = \frac{e \times Q \times \eta \times \ln\left(r/r_1\right)}{2\pi \times h \times \Delta P}, \tag{3}$$

$$e = \frac{\pi \times \left(a^2 - {r_1}^2\right) \times h \times \phi_f}{m_f / \rho}, \tag{4}$$

where a is the principal flow direction; e is the ellipticity, which refers to the relationship of the flow front along the x–y axis; h is the mold thickness; m_f is the injection weight of the resin; Q is the flow rate; r is the flow front radius; r_1 is the hole radius of the injection hole; η is the viscosity; ϕ_f is the porosity; ΔP is the pressure drop; and ρ is the fluid density of the tested fluid.

The proposed rapid permeability method was developed as a more time-efficient alternative to the traditional one-dimensional resin flow test and Easyperm methods. VARTM is a stable process. Therefore, the proposed rapid permeability method is capable to achieve a high level of

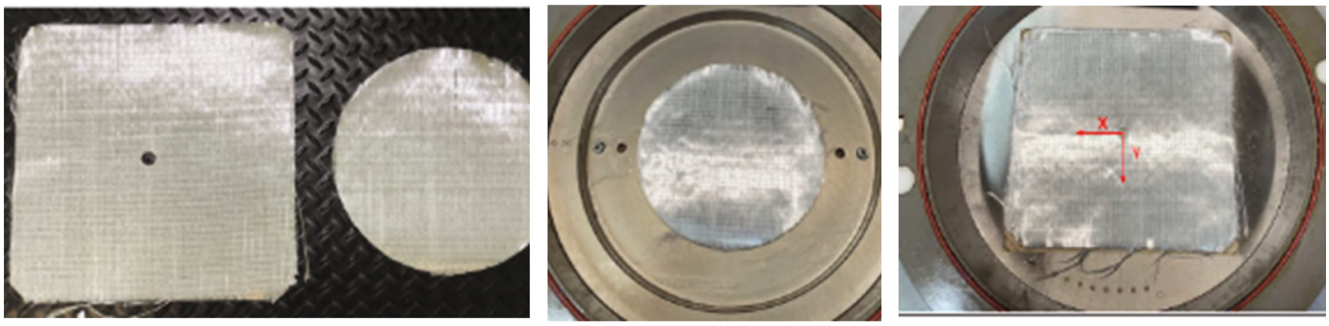

Figure 1: Permeability test conducted with Easyperm. Non-crimp fabric sample. Thickness-direction measurement. Plane-direction measurement.

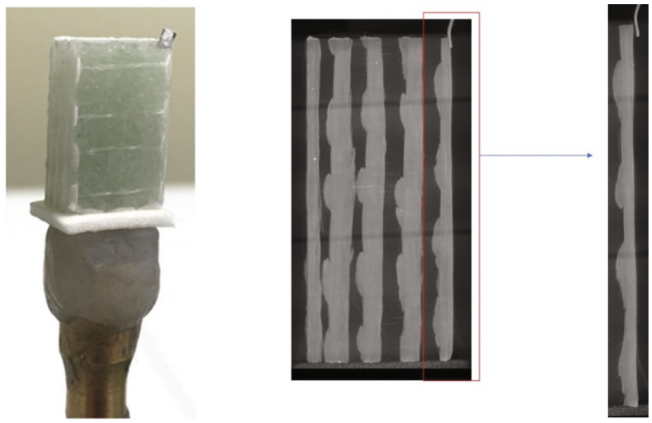

Figure 2: Scanned specimen and low-resolution scanning image.

Table 1: Fiber orientation and area density of LTNM600/P3/600 [33].

Constructions	Area weight (g/m^2)	Tolerance (%)	Material
0°	300	±5	E-Glass 1200 tex
+45°	—	—	—
90°	300	±5	E-Glass 1200 tex
−45°	—	—	—
Core layer	180	±10	Non-woven Core P3
Chopped layer	600	±10	E-Glass 2400 tex
Stitching yarn	16	±5	Polyester 111 dtex
Total area weight	1396	±5	—

product consistency under a given set of lamination conditions. A CT scan was used to assess the stacking status of a fabric in the thickness direction, and the TDSs of fabrics were used to construct a three-dimensional stacking model. Finally, the FlowDict module in GeoDict was used to estimate the permeability of various fabric layups.

For CT scan image processing, the Instarecon and GPU Nrecon software programs were used to perform image reconstruction. Each reconstructed cross section was then reoriented, and a data viewer was used to filter the regions of interest. The images of thickness sections were used as references for constructing three-dimensional models in GeoDict.

The WeaveGeo and FiberGeo modules in GeoDict were used to draw three-dimensional model of the fabrics. As fabrics exhibit compaction behavior under vacuum compression conditions, we first converted multilayer fabrics into FRP test specimens through VARTM and then obtained CT scans of the test specimens in order to obtain the stacking image in the thickness direction. Figure 2 displays a scanned specimen and its low-resolution CT scan pattern. The size of the scanned sample is $5\,mm \times 9\,mm \times 10\,mm$. The main purpose of capturing photos and CT scans was to verify the photograph ability and image resolution of each test specimen. Afterward, we will apply the same test specimen format but adopt a pixel resolution of 2–4 μm for three-dimensional scanning to obtain a high-resolution profile image in the thickness direction.

3. Parameter Validation and Comparison

To assess the accuracy of the proposed rapid permeability estimation method, three types of NCFs that are widely used in FRP boats and FRP parts of wind turbines were selected for testing and comparison in the present study: the orthotropic biaxial core combination fabric LTNM600/P3/600, quadriaxial fabric QX1800/M225, and orthotropic biaxial

Table 2: Fiber orientation and area density of QX1800/M225 [34].

Layer construction	Areal-weight (g/m^2)	Tolerance (g/m^2)	Material type	Sizing type	Tex value (tex)	Filament diameter (μm)	Resin compatibility
			Upper side				
0°	434	±22	E6-glass	320	1103	17	UP, EP, and VE
+45°	458	±23	E6-glass	320	600	17	UP, EP, and VE
90°	472	±24	E6-glass	320	1200	17	UP, EP, and VE
−45°	458	±23	E6-glass	320	600	17	UP, EP, and VE
CSM	225	±18	E6-glass	512	2400	12	UP, EP, and VE

Table 3: Fiber orientation and area density of LT800/M225 [35].

Layer construction	Areal-weight (g/m^2)	Tolerance (g/m^2)	Material type	Sizing type	Tex value (tex)	Filament diameter (μm)	Resin compatibility
			Upper side				
0°	402	±21	E6-glass	320	1460	20	UP, EP, and VE
90°	402	±21	E6-glass	320	600	17	UP, EP, and VE
Chop mat	225	±18	E6-glass	520	2400	13	UP, EP, and VE

Table 4: Average parameters obtained using one-dimensional resin flow tests and Easyperm.

NCF types	Thickness (mm)	Porosity (%)	K_x (m^2)	K_y (m^2)	K_z (m^2)
LT800/M225	3.02	45.77	2.82×10^{-11}	2.82×10^{-11}	2.10×10^{-12}
QX1800/M225	5.68	43.33	3.16×10^{-11}	3.16×10^{-11}	2.17×10^{-12}
LTNM600/P3/600	7.32	70.23	4.51×10^{-10}	4.51×10^{-10}	5.47×10^{-12}

fabric LT800/M225. The TDSs of these NCFs are presented in Tables 1, 2, and 3.

NCF multiaxial reinforcements are multilayer fabrics with a single axial orientation. They can be used along with polypropylene flow media or chopped strand mat to accelerate resin flow. The porosity of NCF fabrics is inconsistent. Tables 1, 2, and 3 reveal that the tolerance of the selected NCFs can reach maximum 20% (weight per unit area) and minimum 5%, which means porosity variations affect the consistency and accuracy of permeability measurements.

In the present study, each selected NCF was comprised of four layers (stacking number = 4). The one-dimensional flow test and Easyperm were used to estimate the porosity and permeability of the fabrics, which then served as benchmarks for subsequent comparisons. The TDSs of the three selected NCFs indicate that the weight variations of single-layer fabrics can reach ±5%; that is, the extreme weight variation of the selected NCFs can reach 10%. When the thicknesses of the three NCFs were measured under vacuum conditions, the variation between the maximum and minimum thicknesses was approximately 10%, regardless of whether the thickness of the fabrics was measured using the one-dimensional resin flow test or Easyperm. In addition, the relationship between porosity and thickness was revealed to be nonlinear. Take four layers of QX1800/M225 on Table 4 as an example, when the ±5% weight variations of the NCFs were substituted into equation (1), the results revealed porosity variations of up to 14%. Given the state of current NCF manufacturing technology, such variations are unavoidable. Therefore, when traditional methods are applied to measure porosity and permeability, lamination thickness must be measured at multiple points, and the measured results must be averaged. The differences of measured points also affect the final porosity and permeability estimation results.

The thickness parameters obtained using the one-dimensional resin flow test and Easyperm were separately used to estimate porosity. Specifically, the thickness parameters were averaged to obtain the average porosity, which was used as the basis for subsequent permeability calculations. Two sets of one-dimensional resin flow tests were conducted on each NCF. The slope m is the square of the resin flow front versus the resin flow time for each test set. The average value of m was substituted into equation (2) to obtain the average permeability.

Easyperm was also used to estimate permeability. The sensor nodes of Easyperm can only be set at the bottom and top of a test fabric. When Easyperm was used to estimate permeability, the pressure difference between the bottom and top sensor nodes was affected by the presence of unidirectional fibers in each layer. Consequently, the measurement errors pertaining to K_x and K_y (i.e., permeability in the plane direction) were >20%. Overall, the results indicate that Easyperm is unsuitable for measuring the permeability of materials that exhibit macroscopic inhomogeneity

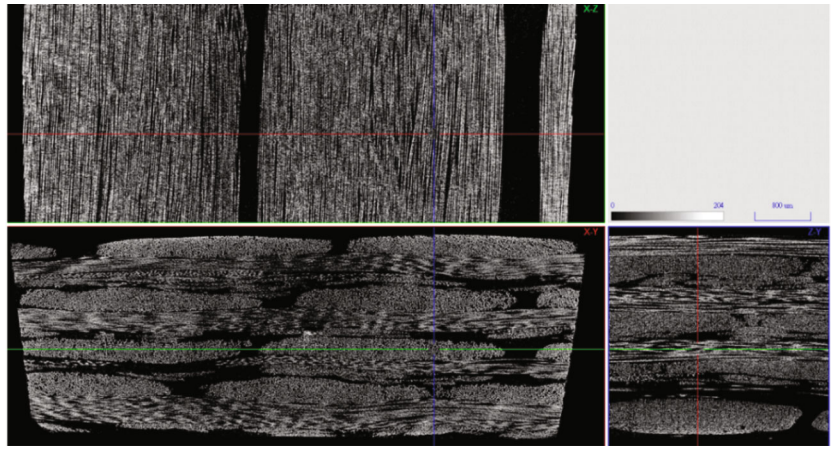

(a)

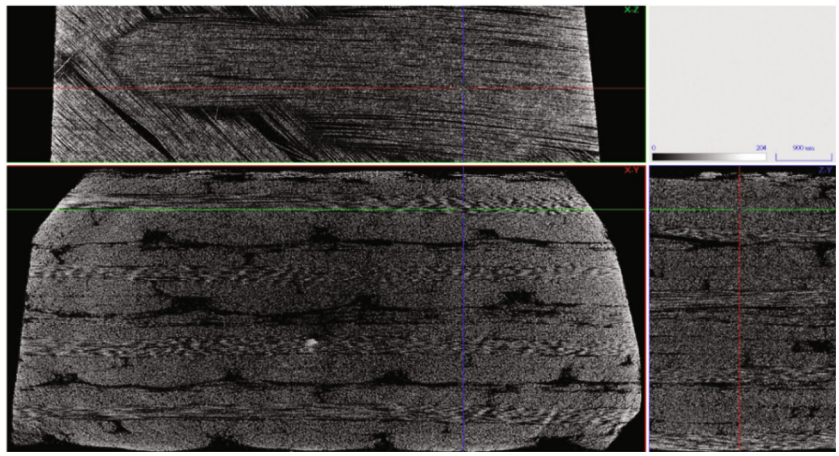

(b)

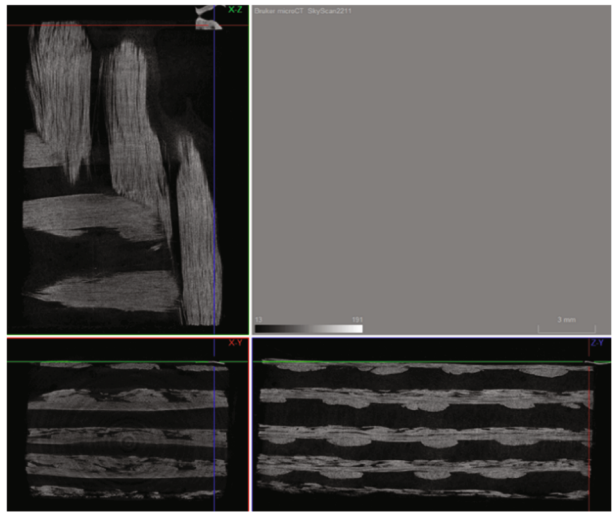

(c)

Figure 3: CT Scan three-view results. (a) CT scan three-view results for LT800/M225. (b) CT scan three-view results for QX1800/M225. (c) CT scan three-view results for LTNM600/P3/600.

in the thickness direction. Because NCFs exhibit such inhomogeneity, a change in the composition sequence in the fiber weaving direction can theoretically influence pressure, which in turn affects the measurement of K_z. However, the results of the present study indicate that the permeability variation in the thickness direction was not prominent when the examined fabric was thin. In this paper, the variations for multiple measurements were all <10%.

Given the prominent errors pertaining to the Easyperm-derived K_x and K_y results, the values of K_x and K_y should be

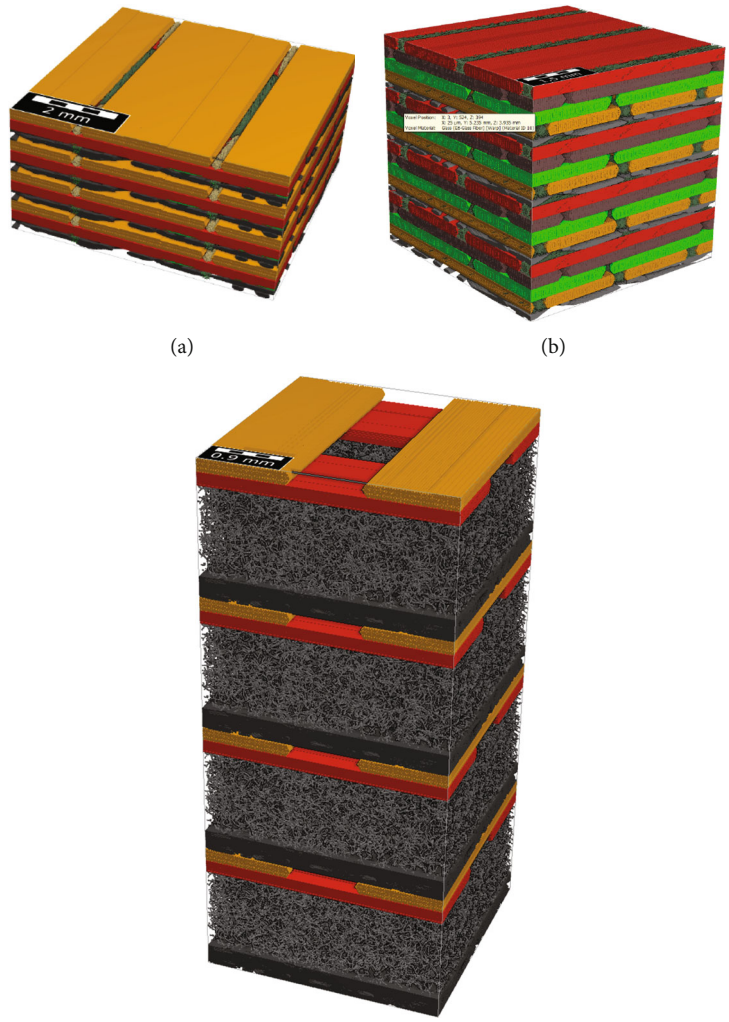

(a) (b) (c)

Figure 4: Three-dimensional stacking models constructed using GeoDict. (a) LT800/M225. (b) QX1800/M225. (c) LTNM600/P3/600.

based on the results of one-dimensional flow tests. However, the permeability in the thickness direction could not be obtained through one-dimensional resin flow tests. Therefore, under the condition that the measurement variation must be <10%, the permeability K_z in the thickness direction was obtained as the average K_z value measured using Easyperm. Table 4 lists the average thickness, porosity, and permeability of the three examined NCFs when the stacking number was 4.

The proposed rapid estimation method was applied to estimate the porosity and permeability of the three NCFs. Figures 3(a), 3(b), and 3(c) present the CT scan three-view results for LT800/M225, QX1800/M225, and LTNM600/P3/600. From these results, the fabric configurations of the three NCFs in the plane and thickness directions were obtained. On the basis of the TDSs and captured CT scans, three-dimensional models of the laminates were constructed using GeoDict (Figure 4). FlowDict was used to simulate the porosity and permeability of the three NCFs in the horizontal and thickness directions. The FlowDict simulation process is illustrated in Figure 5.

The porosity and permeability parameters obtained using the FlowDict module are listed in Table 5. A comparison of the FlowDict-derived results and those presented in Table 4 revealed that the variations in the K_x and K_y (in-plane permeability) values of the three NCFs were not prominent. However, when the proposed rapid permeability method was applied, the permeability variations in these values became prominent; that is, the actual conditions of the NCFs were more accurately reflected when using the proposed method than when using the other two methods. For the permeability in the thickness direction, the variations between the values estimated using the proposed method and those measured using Easyperm ranged between 20% and 50%. This phenomenon can be attributed to the inconsistent thickness measurements obtained using Easyperm under vacuum conditions.

However, when VARTM was used to infuse large components, the flow distances of the resin in the x-direction and y-direction were considerably greater than that in the thickness direction. At this point, the resin flow front was mainly influenced by the permeability in the x-direction

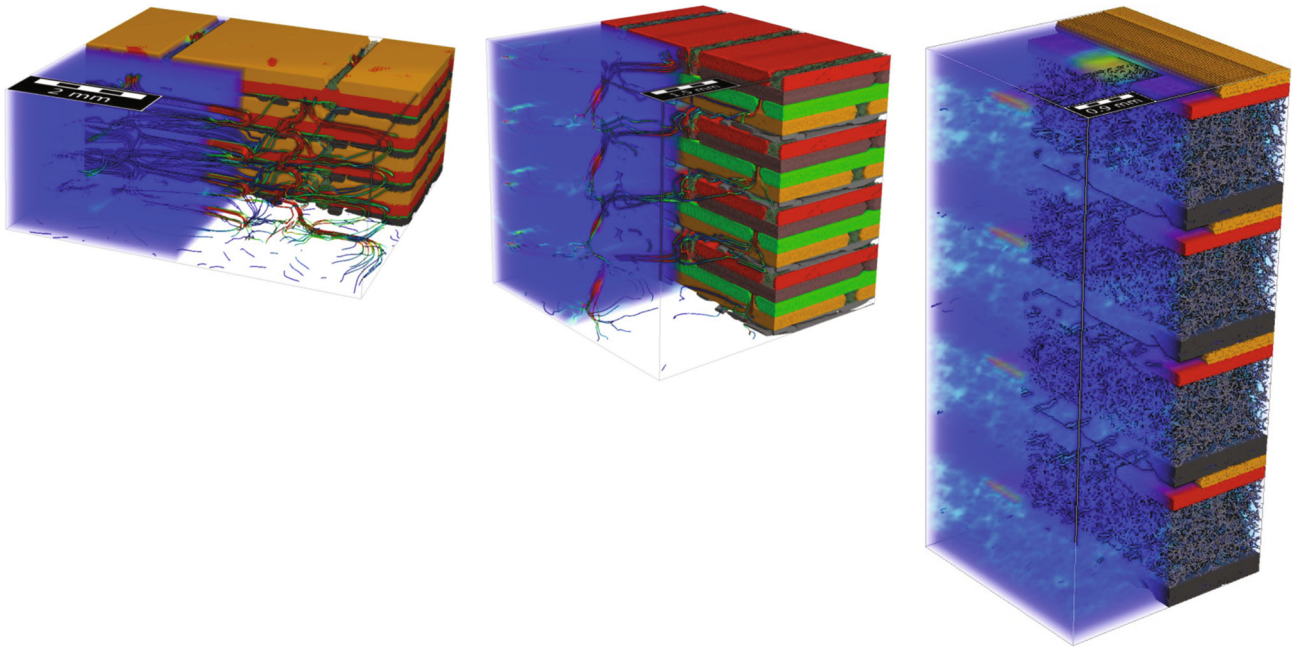

(a) (b) (c)

Figure 5: Flow simulation process in FlowDict. (a) LT800/M225. (b) QX1800/M225. (c) LTNM600/P3/600.

Table 5: Simulated permeability and porosity obtained using GeoDict.

NCF types	Porosity (%)	K_x (m^2)	K_y (m^2)	K_z (m^2)
LT800/M225	44.8	2.631×10^{-11}	2.957×10^{-11}	1.75×10^{-12}
QX1800/M225	41.9	3.546×10^{-11}	3.126×10^{-11}	1.299×10^{-12}
LTNM600/P3/600	72.2	3.749×10^{-10}	3.756×10^{-10}	9.16×10^{-12}

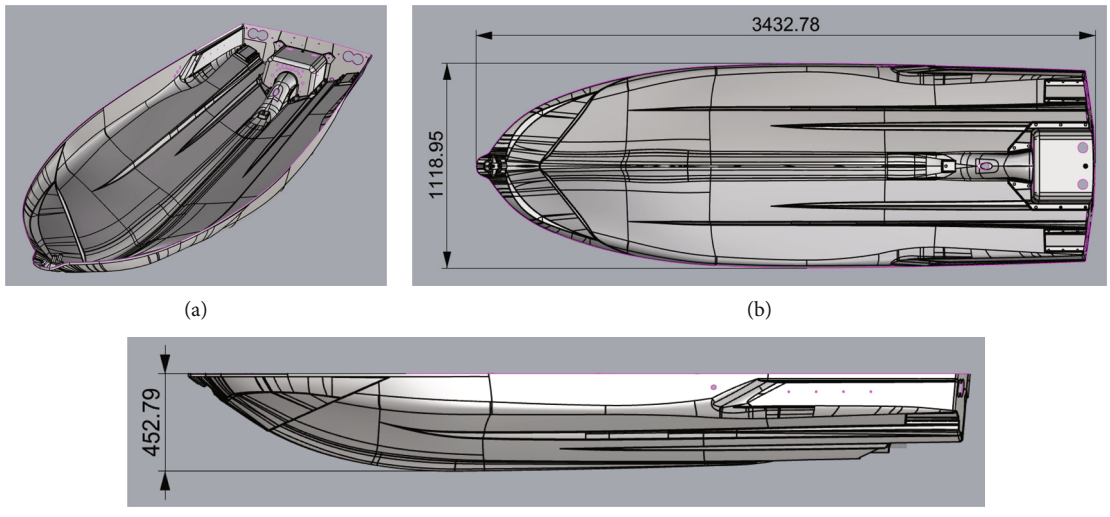

(a) (b) (c)

Figure 6: Three-dimensional model of a PWC. (a) Isometric view. (b) Top view. (c) Side view.

and y-direction. Although the thickness-direction permeability values obtained through the various estimation methods exhibited several errors, we used a PWC hull to verify that the variations in K_z did not considerably affect the overall flow front estimations when the order of the thickness-direction permeability K_z remained unchanged.

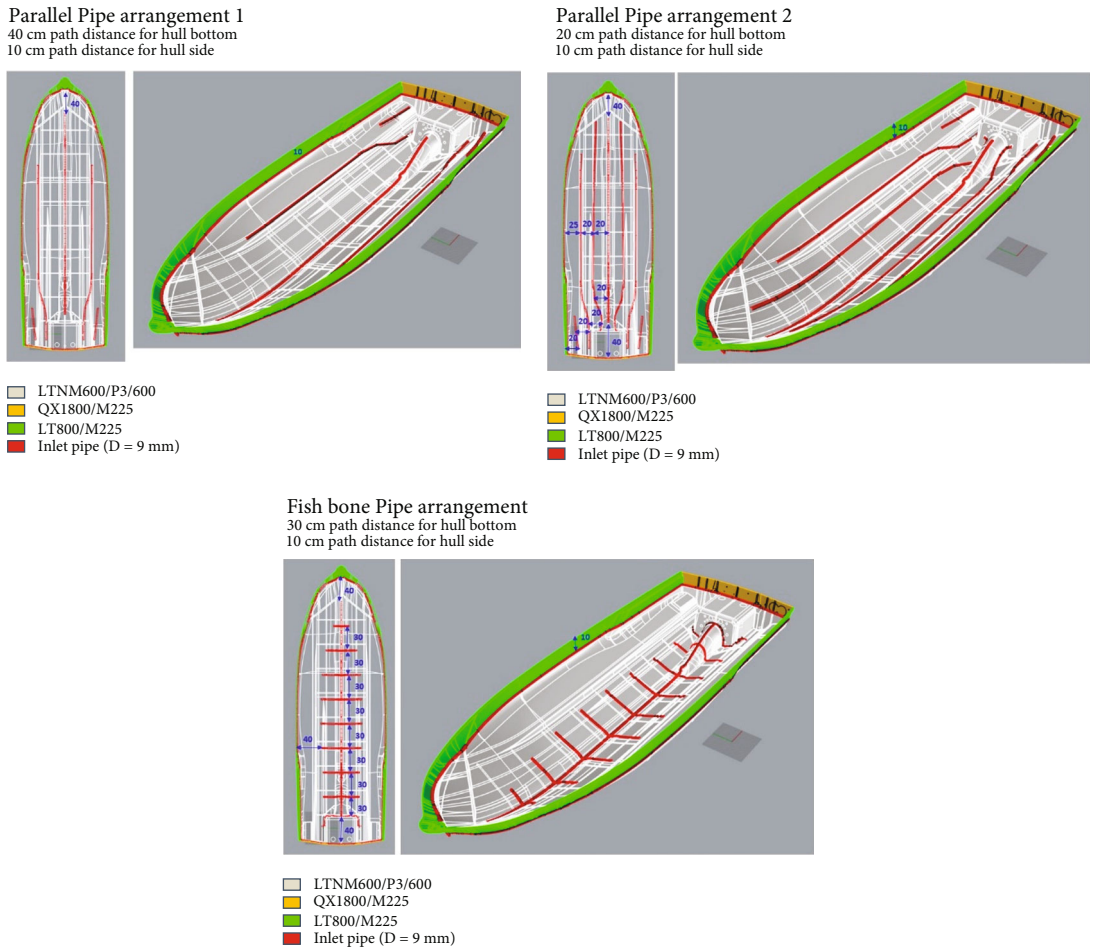

Figure 7: Pipe arrangement. Case I: parallel pipe arrangement 1. Case II: parallel pipe arrangement 2. Case III: fishbone pipe arrangement.

Table 6: Filling time required for the three pipe arrangements.

Pipe arrangement type	Simulation filling time (s)
Parallel pipe arrangement 1	1177
Parallel pipe arrangement 2	882
Fishbone pipe arrangement	936

In summary, the proposed rapid estimation method considerably reduced the frequency with which permeability measurement tests had to be performed. On the basis of only the TDS and CT scan results for the fabrics, their permeability and porosity could be accurately obtained provided that a specific number of layers was examined. Compared with the commonly used one-dimensional flow test and Easyperm methods, the proposed estimation method takes less time and is more reliable. Furthermore, the proposed method meets the practical needs of various industries.

4. Infusion Verification of a PWC Hull Mold

To verify whether the permeability and porosity obtained using the proposed rapid estimation method were sufficiently accurate for application in the 3D mold flow analysis of large FRP components, we used a PWC hull as the verification target and compared the infusion results obtained through VARTM with those obtained through mold flow analysis. We substituted the permeability and porosity obtained through FlowDict into Moldex3D to perform 3D mold flow analysis. First, we compared the infusion time required for various pipe arrangements, after which we selected the appropriate pipe arrangement for the actual infusion conducted on the PWC hull.

The PWC hull mold used in the presented study was donated by Belassi GmbH. This PWC hull had a length, width, and depth of 3.5, 1.1, and 0.5 m, respectively (Figure 6). The PWC hull had numerous bending sections that exhibited continuous bending angles and bent radii, which increased the difficulty of performing fabrics layup. When a fabric cannot be completely fit on the surface of a mold, additional channels are created to accelerate resin flow. This phenomenon is called the bridge effect, and it causes mold flow analysis results and actual infusion results to differ considerably. To avoid this phenomenon, a focus of the present study was to ensure that the examined fabrics fit tightly onto the mold surface.

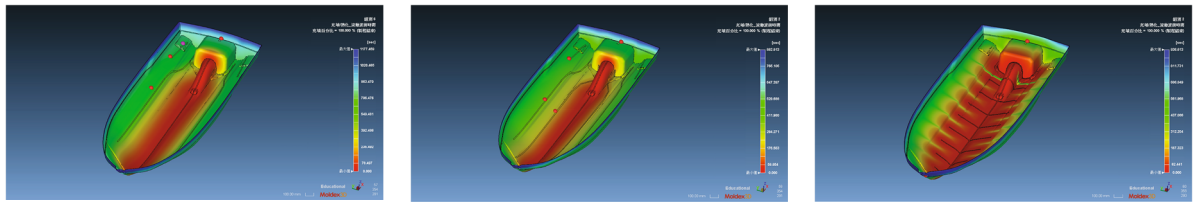

(a) (b) (c)

Figure 8: Mold flow simulation results for the three pipe arrangements. (a) Parallel pipe arrangement 1. (b) Parallel pipe arrangement 2. (c) Fishbone pipe arrangement.

Table 7: Comparison of the mold flow analysis and actual filling results.

	Actual filling time (s)	Simulation filling time (s)	Error (%)
Initial	0	0	—
The second pipe	634	636	−0.31
The third pipe	784	724	7.65
The fourth pipe	936	887	5.23
Complete	1264	1174	6.88

The three examined NCFs were laminated without distribution media in various areas of the PWC hull. Four layers of LT800/M225 were laminated on the side plate, four layers of LTNM600/P3/600 were laminated on the bottom plate, and four layers of QX1800/M225 were laminated on the stern plate. In addition, two parallel resin pipe arrangements and one fishbone resin pipe arrangement were selected for mold flow analysis under the same lamination conditions to determine the optimal infusion conditions. The layouts and pipe arrangements of the fabrics are displayed in Figure 7. Resin inlet pipes are presented in red lines. For clarity, the first, second, and third pipe arrangements are referred to as parallel pipe arrangement 1, parallel pipe arrangement 2, and the fishbone pipe arrangement, respectively.

Moldex3D and the permeability and porosity parameters listed in Table 5 were used for 3D mold flow analysis. The estimated infusion completion times for the three types of pipe arrangements are listed in Table 6, and the mold flow analysis results are displayed in Figure 8. In general, the time required for the infusion of large FRP components during resin curing was approximately between 30 minutes and 2 hours. The mold flow analysis results reveal that the infusion process for each of the three types of pipe arrangements examined in this study was completed within 20 minutes. No matter the infusion was completed in 882 seconds or 1177 seconds, the minimum gelation time for both is 30 minutes. Workers have to stick to the position until resin gelation. Although an increase in the number of feeding pipes reduces the infusion time, it also caused an increase in the working hours of the pipe arrangements, the quantity of pipe consumables required, and quantity of resin consumed in the pipes.

On the basis of practical and rational considerations with respect to pipe arrangements, parallel pipe arrangement 1 (Figure 8(a)) was selected as the pipe arrangement for PWC hull infusion. Subsequently, the obtained PWC hull infusion results were compared with the mold flow analysis results.

In parallel pipe arrangement 1 (Figure 8(a)), four feed pipes are used (i.e., one at the center of the hull bottom, one at the center of the hull side, one on the two sides of the hull side, and one at the geometric protrusion at the front of the transom). The filling time measured from the resin flow front to the corresponding feed pipe was the basis for comparing the mold flow analysis and PWC hull infusion results.

The viscosity of the resin during infusion was 260 cps, and the vacuum pressure was 0.1 MPa (1 bar). The comparison of the mold flow analysis and hull infusion results (Table 7) revealed that all the variations between the time required for resin to flow to the relevant feeding pipe (i.e., hull infusion results) and the corresponding resin flow time observed in the mold flow analysis results were within 10%. These variation results are similar to the fabric pore variability that derived from manufacturing. Therefore, the analysis variation range was acceptable. This finding also confirms that the proposed permeability estimation method, which involves the combined use of fabric TDSs and CT scans, is accurate.

Comparisons of the resin flow fronts obtained in the mold flow analysis and hull infusion test are presented in Figures 9, 10, and 11. These comparisons reveal that the resin flow front flowing from the feed pipe at the bottom of the hull to the two hull sides was consistent between the mold flow analysis and hull infusion test. Moreover, the time required by the resin flow front to flow through the second pipe in the hull infusion test was identical to that obtained in the mold flow analysis. Figure 10 reveals that when the resin flowed through the second pipe, the resin flow front on the right side of the hull flowed slightly behind the resin flow front on the left side of the hull. This phenomenon, which also occurs during infusion in practice, may be caused by the fabric layup or the pore variability of the fabrics that derived from manufacturing. However, the aforementioned phenomenon generally does not have a noticeable effect on infusion variation. For the time required for the resin to flow to the third pipe, the variation between the hull infusion and mold flow analysis results was only 7.65%.

Given that several geometric shapes are present at the front of the transom, short feeding pipes (the fourth pipe) were also positioned in various areas. Figure 11 presents a comparison of the hull infusion and mold flow analysis

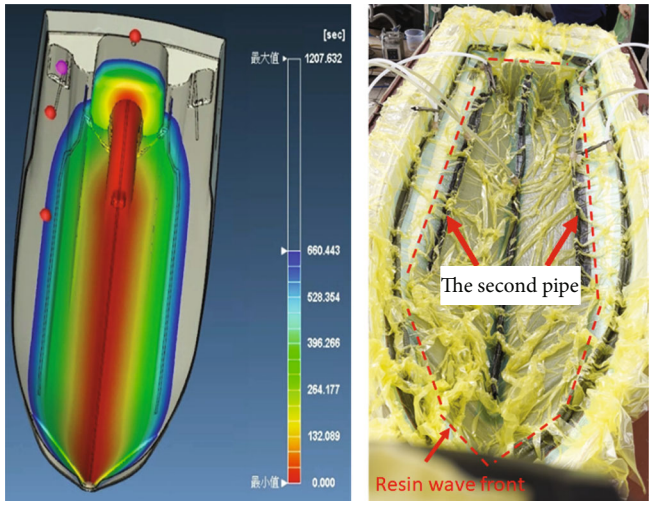

Figure 9: Comparison of the resin flow front along the second pipe.

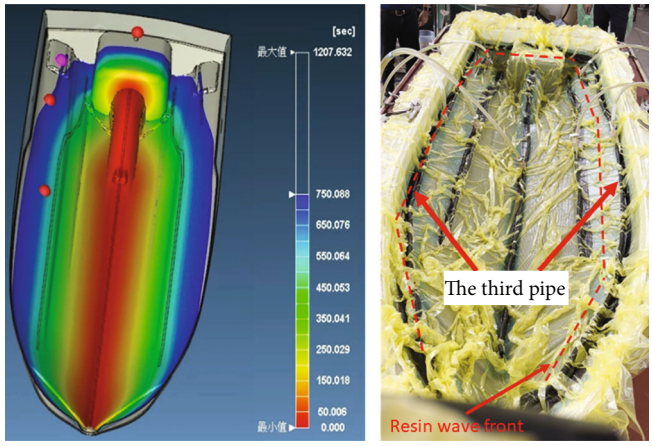

Figure 10: Comparison of the resin flow front along the third pipe.

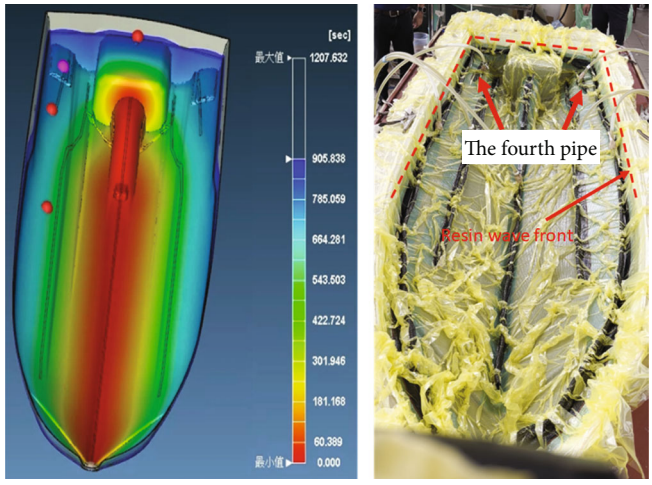

Figure 11: Comparison of the resin flow front along the fourth pipe.

results for the flow of the resin flow front to the fourth pipe. At this point, the infusion on the two hull sides of the hull had already been completed; however, the infusion on the stern plate was ongoing. The mold flow analysis results were consistent with the practical hull infusion results; specifically, the variation between them was 5.23%. The time required to complete the infusion was 1174 seconds in the final mold flow analysis and 1264 seconds in the practical hull infusion test; thus, these results were similar.

5. Conclusion

In this paper, a rather rapid and effective method is proposed for estimating the permeability and porosity of laminated fabrics. The proposed rapid permeability method does not need to conduct traditional permeability measurement tests, such as one-dimensional resin flow test, which usually take 1 week to get optimized resin pipe arrangement; instead, with only the TDSs of the applied fabrics and CT scan results, three-dimensional models of FRP laminations can be constructed in GeoDict, which merely takes a single day to get optimized resin pipe arrangement. The results obtained using the proposed rapid permeability method were successfully applied to predict the porosity and permeability of various fabrics, and the obtained parameters were consistent with the measurement results obtained using the traditional one-dimensional resin flow test and Easyperm method. Therefore, by using the proposed rapid permeability method, optimized resin pipe arrangement can be acquired in a single day, which is highly practical for application in various industries.

In addition, Moldex3D was used to simulate the resin flow of a PWC hull during VARTM. The input parameters for permeability and porosity used in the Moldex3D model were obtained using the proposed rapid permeability method. The comparisons of the simulation results and hull infusion results revealed that the variations in the resin flow front were <8%. The results of the present study indicate that Moldex3D can accurately simulate the resin flow conditions in large FRP components. For the manufacturing of wind turbine blades and other related large FRP components, the proposed rapid estimation method can be used in the planning of pipe arrangements and in preliminary evaluations.

Data Availability

Data supporting this research article are available from the corresponding author or first author on reasonable request.

Conflicts of Interest

The authors declare that they have no conflicts of interest.

Acknowledgments

We thank CoreTech System Co., Ltd. for the Moldex3D-related support that they provided and Belassi Co. of Austria for donating the PWC hull mold used in this study.

References

[1] G. Struzziero and J. J. E. Teuwen, "Effect of convection coefficient and thickness on optimal cure cycles for the manufacturing of wind turbine components using VARTM," *Composites. Part A, Applied Science and Manufacturing*, vol. 123, pp. 25–36, 2019.

[2] Y. Aoki, Y. Hirano, S. Sugimoto, Y. Iwahori, Y. Nagao, and T. Ohnuki, "Durability and damage tolerance evaluation of VaRTM composite wing structure," in *ICAF 2011 Structural Integrity: Influence of Efficiency and Green Imperatives*, pp. 1–3, This is conference paper which was 26th ICAF Symposium – Montreal, Netherlands, 2011.

[3] M. Bodaghi, S. V. Lomov, P. Simacek, N. C. Correia, and S. G. Advani, "On the variability of permeability induced by reinforcement distortions and dual scale flow in liquid composite moulding: a review," *Composites. Part A, Applied Science and Manufacturing*, vol. 120, pp. 188–210, 2019.

[4] R. S. Parnas, J. G. Howard, T. L. Luce, and S. G. Advani, "Permeability characterization. Part 1: a proposed standard reference fabric for permeability," *Polymer Composites*, vol. 16, no. 6, pp. 429–445, 1995.

[5] S. Amico and C. Lekakou, "An experimental study of the permeability and capillary pressure in resin-transfer moulding," *Composites Science and Technology*, vol. 61, no. 13, pp. 1945–1959, 2001.

[6] H. Tan and K. M. Pillai, "Multiscale modeling of unsaturated flow in dual-scale fiber preforms of liquid composite molding I: isothermal flows," *Composites. Part A, Applied Science and Manufacturing*, vol. 43, no. 1, pp. 1–13, 2012.

[7] A. Nabovati, E. W. Llewellin, and A. C. M. Sousa, "Through-thickness permeability prediction of three-dimensional multifilament woven fabrics," *Composites. Part A, Applied Science and Manufacturing*, vol. 41, no. 4, pp. 453–463, 2010.

[8] Q. Wang, B. Mazé, H. V. Tafreshi, and B. Pourdeyhimi, "A note on permeability simulation of multifilament woven fabrics," *Chemical Engineering Science*, vol. 61, no. 24, pp. 8085–8088, 2006.

[9] A. Endruweit, T. Luthy, and P. Ermanni, "Investigation of the influence of textile compression on the out-of-plane permeability of a bidirectional glass fiber fabric," *Polymer Composites*, vol. 23, no. 4, pp. 538–554, 2002.

[10] K. Han, S. Jiang, C. Zhang, and B. Wang, "Flow modeling and simulation of SCRIMP for composites manufacturing," *Composites. Part A, Applied Science and Manufacturing*, vol. 31, no. 1, pp. 79–86, 2000.

[11] M. K. Kang, W. I. Lee, and H. T. Hahn, "Analysis of vacuum bag resin transfer molding process," *Composites. Part A, Applied Science and Manufacturing*, vol. 32, no. 11, pp. 1553–1560, 2001.

[12] N. C. Correia, F. Robitaille, A. C. Long, C. D. Rudd, P. Šimáček, and S. G. Advani, "Analysis of the vacuum infusion moulding process: I. Analytical formulation," *Composites. Part A, Applied Science and Manufacturing*, vol. 36, no. 12, pp. 1645–1656, 2005.

[13] M. J. Buntain and S. Bickerton, "Compression flow permeability measurement: a continuous technique," *Composites. Part A, Applied Science and Manufacturing*, vol. 34, no. 5, pp. 445–457, 2003.

[14] Q. Govignon, S. Bickerton, J. Morris, and P. A. Kelly, "Full field monitoring of the resin flow and laminate properties during the resin infusion process," *Composites. Part A, Applied Science and Manufacturing*, vol. 39, no. 9, pp. 1412–1426, 2008.

[15] J. Mogavero and S. G. Advani, "Experimental investigation of flow through multi-layered preforms," *Polymer Composites*, vol. 18, no. 5, pp. 649–655, 1997.

[16] B. Caglar, G. Broggi, M. A. Ali, L. Orgéas, and V. Michaud, "Deep learning accelerated prediction of the permeability of fibrous microstructures," *Composites. Part A, Applied Science and Manufacturing*, vol. 158, p. 106973, 2022.

[17] R. Arbter, J. M. Beraud, C. Binetruy et al., "Experimental determination of the permeability of textiles: a benchmark exercise," *Composites. Part A, Applied Science and Manufacturing*, vol. 42, no. 9, pp. 1157–1168, 2011.

[18] Q. Liu, R. S. Parnas, and H. S. Giffard, "New set-up for in-plane permeability measurement," *Composites. Part A, Applied Science and Manufacturing*, vol. 38, no. 3, pp. 954–962, 2007.

[19] T. H. Chiu, J. B. Li, Y. Yao et al., "Estimation of local permeability/porosity ratio in resin transfer molding," *Journal of the Taiwan Institute of Chemical Engineers*, vol. 91, pp. 32–37, 2018.

[20] B. J. Wei, Y. C. Chuang, K. H. Wang, and Y. Yao, "Model-assisted control of flow front in resin transfer molding based on real-time estimation of permeability/porosity ratio," *Polymer Journal*, vol. 8, no. 9, p. 337, 2016.

[21] F. V. Härter, J. A. Souza, L. A. Isoldi, E. D. D. Santos, and S. C. Amico, "Transverse permeability determination and influence in resin flow through an orthotropic medium in the RTM process," *Matéria*, vol. 22, no. 2, 2017.

[22] F. Trochu, R. Gauvin, D. M. Gao, and J. F. Boudreault, "RTMFLOT- an integrated software environment for the computer simulation of the resin transfer molding process," *Journal of Reinforced Plastics and Composites*, vol. 13, no. 3, pp. 262–270, 1994.

[23] C. Dong, "An equivalent medium method for the vacuum assisted resin transfer molding process simulation," *Composites. Part A, Applied Science and Manufacturing*, vol. 40, no. 13, pp. 1193–1212, 2006.

[24] Y. De Parseval, K. M. Pillai, and S. G. Advani, "A simple model for the variation of permeability due to partial saturation in dual scale porous media," *Transport in Porous Media*, vol. 27, no. 3, pp. 243–264, 1997.

[25] D. Droste, L. Krishnappa, S. Bornemann et al., "Investigation of the compaction behaviour of a quasi-unidirectional non-crimp fabric during the vacuum infusion process," *Journal of Composite Materials*, vol. 56, no. 16, pp. 2509–2524, 2022.

[26] M. Bodaghi, A. Vanaerschot, S. V. Lomov, and N. C. Correia, "On the stochastic variations of intra-tow permeability induced by internal geometry variability in a 2/2 twill carbon fabric," *Composites. Part A, Applied Science and Manufacturing*, vol. 101, pp. 444–458, 2017.

[27] E. Rodriguez, F. Giacomelli, and A. Vazquez, "Permeability-porosity relationship in RTM for different fiberglass and natural reinforcements," *Journal of Composite Materials*, vol. 38, no. 3, pp. 259–268, 2004.

[28] C. Dong, "Development of a process model for the vacuum assisted resin transfer molding simulation by the response surface method," *Composites. Part A, Applied Science and Manufacturing*, vol. 37, no. 9, pp. 1316–1324, 2006.

[29] N. Vernet, E. Ruiz, S. Advani et al., "Experimental determination of the permeability of engineering textiles: benchmark II," *Composites. Part A, Applied Science and Manufacturing*, vol. 61, no. 9, pp. 172–184, 2014.

[30] J. H. Wu, C. H. Chung, K. L. Chen et al., "Experimental study on flow properties of resins in VARTM used in shiphull building," *Journal of Taiwan Society of Naval Architects and Marine Engineers*, vol. 25, pp. 107–115, 2006.

[31] Y. H. Lai, B. Khomami, and J. K. Kardos, "Accurate permeability characterization of preforms used in polymer matrix composite fabrication processes," *Polymer Composites*, vol. 18, no. 3, pp. 368–377, 1997.

[32] H. M. El-Dessouky, A. E. Snape, R. J. Scaife et al., "Design, weaving and manufacture of a large 3D composite structures for automotive applications," in *3D Fabrics & Their Applications Conference*, pp. 8–9, Conference Organising Committee, The 9th World Conference in 3D Fabrics and Their Applications, Roubaix (France), 2016, September.

[33] LTNM600/P3/600 TDS, NMG Composites CO., LTD. 2015 December. 8. https://www.carbon-core.com/pdfs/core-combination/LTNM600-P3-600.pdf.

[34] E-LT800/M225-320 product Description, Document no. CPS0194000 REV.A, Hengshi Fiberglass Fabrics Co., Ltd.

[35] E-QX1800/M225-320 product Description, Document no. CPS0381000 REV.A, Hengshi Fiberglass Fabrics Co., Ltd.